

Coupled reaction kinetics of duplex steelmaking process for high phosphorus hot metal

Xie ZHANG¹⁾, Bing XIE¹⁾, Jiang DIAO²⁾ and Chengqing JI¹⁾

1) College of Materials Science and Engineering, Chongqing University, Chongqing 400044, P. R. China

2) CISDI Engineering CO. LTD, Chongqing 400000, China

Abstract: Duplex steelmaking process has been proven to be an effective solution for the utilization of high phosphorus iron ore, yet systematic analyses of the dephosphorization rate and mechanism of duplex melting for high phosphorus hot metal were seldom reported. In the present work, based on the kinetic model proposed by Robertson, a modified coupled reaction kinetic model was formulated firstly. Moreover, the dephosphorization process of duplex melting for high phosphorus hot metal was analyzed by the established model. A series of experiments were carried out to validate the accuracy of the established model and the calculated results showed a good agreement with the experimental data. Effects of components of both hot metal and slag on the interfacial oxygen activity during dephosphorization were discussed. It was found that a higher content of FeO in slag and lower concentration of C, Si and Mn in hot metal would contribute to a larger value of interfacial oxygen activity. The results indicate that the concentration of Si in the high phosphorus hot metal should be limited at an appropriate value due to the period of dephosphorization is relatively long and the oxidation of silicon is prior to that of phosphorus. Some parametric study was conducted to make a further discussion of the mechanism of duplex steelmaking process for high phosphorus hot metal.

Keywords: High phosphorus hot metal, duplex melting process, coupled reaction kinetics

1. Introduction

Recently, much attention has been paid to the utilization of iron ore with low content of iron due to the remarkable rise in the price of iron ore and the gradual exhaustion of iron ore resources. As a typical and significant iron ore resource, the high phosphorus iron ore plays a vital role under this background. However, it is widely accepted that phosphorus is a harmful element for most steel product. Therefore, the development of effective dephosphorization method is a key point in the utilization of high phosphorus iron ore.

The duplex steelmaking process originated in Japan has been proven to be a valid way to treat the phosphorus in hot metal and is schematically illustrated in Fig.1. Although the duplex melting process adopted by the metallurgical engineers in Japan is mainly focused on the production of ultra-low phosphorus steel, yet this idea has inspired us to use it as an effective solution for the dephosphorization of high phosphorus hot metal produced from high phosphorus iron ore. After a series of previous research work in both lab and steel plant, duplex steelmaking process has been turned out to be suitable for handling this issue of dephosphorization.

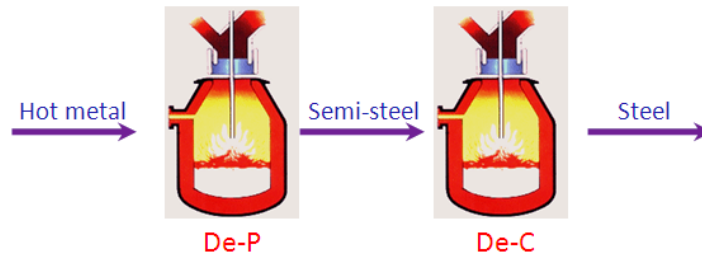


Fig.1 Schematic of duplex steelmaking process

Nonetheless, this process has never been employed to treat the high phosphorus iron ore on a large scale. Moreover, fundamental research on the dephosphorization process has seldom been conducted and reported. Therefore, fundamental thermodynamic and kinetic analyses of the duplex steelmaking process for high phosphorus hot metal are quite necessary. Based on this background, this work attempts to investigate the dephosphorization process for high phosphorus hot metal based on coupled reaction kinetic model proposed by Robertson *et al.*[1]. Furthermore, a series of experiments were designed and carried out to validate the accuracy of the established model. In addition, some parametric study was conducted to analyze and discuss the mechanism of duplex steelmaking process for high phosphorus hot metal.

2. Modified coupled reaction kinetic model

2.1 Model formulation

Robertson and Ohguchi [1, 2] formulated the coupled reaction kinetic model to analyze both the dephosphorization and desulfurization processes based on the hypothesis that the slag-metal reaction is in equilibrium and the process kinetics are controlled by the mass transfer between slag and metal. The model has been proven to be able to accurately predict the variation of different components during the coupled reactions between slag and metal. Xu [3] and Dong *et al.* [4] extended this model to investigate the kinetics of hot metal pretreatment process. Fu and Zhao *et al.* [5, 6] modified this model and analyzed the oxidizing dephosphorization of stainless steel. Tian [7] made some corrections on this model and used it to probe the deep dephosphorization process of low phosphorus hot metal. In this work, a series of modifications was made to conduct a more accurate analysis of the present research object.

Based on the composition of hot metal and slag, the reactions considered in present study are schematically illustrated in Fig.2 and specifically given by Eqs. (1)-(7).

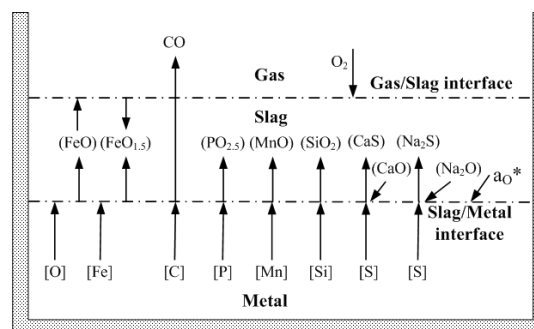


Fig.2 Schematic of reactions model



The oxidation reactions of elements in hot metal can be generally expressed by



Then the equilibrium constant can be defined by

$$K_M = \frac{a_{\text{MO}_x}^*}{a_{\text{M}}^* a_{\text{O}}^{*x}} = \frac{\gamma_{\text{MO}_x} X_{\text{MO}_x}^*}{f_{\text{M}} [\% \text{M}]^* f_{\text{O}}^x [\% \text{O}]^{*x}} \quad (9)$$

In particular, the equilibrium constant of desulfurization is defined by

$$K_S = \frac{a_{\text{MS}}^* a_{\text{O}}^*}{a_{\text{MO}}^* a_{\text{S}}^*} = \frac{\gamma_{\text{MS}} X_{\text{MS}}^* a_{\text{O}}^*}{f_{\text{S}} [\% \text{S}]^* \gamma_{\text{MO}} X_{\text{MO}}^*} \quad (10)$$

The relation between the molar fraction of slag component and its mass fraction can be expressed by

$$X_i = \frac{(\% i) \rho_s}{100 M_i C} \quad (11)$$

The modified equilibrium constant with all units in mass% is referred to as the effective equilibrium constant E_M and is generally expressed as follows.

$$E_M = \frac{(\% \text{MO}_x)^*}{[\% \text{M}]^* a_{\text{O}}^{*x}} = \frac{100 C M_{\text{MO}_x} f_{\text{M}} K_M}{\rho_s \gamma_{\text{MO}_x}} \quad (12)$$

In addition, the effective equilibrium constants of decarburization and desulfurization can be illustrated respectively by

$$E_C = \frac{p_{\text{CO}}^*}{[\% \text{C}]^* a_{\text{O}}^*} = f_{\text{C}} K_C \quad (13)$$

$$E_S = \frac{(\% \text{MS})^* a_{\text{O}}^*}{[\% \text{S}]^* (\% \text{MO})^*} = \frac{M_{\text{MS}} f_{\text{S}} \gamma_{\text{MO}} K_S}{M_{\text{MO}} \gamma_{\text{MS}}} \quad (14)$$

During the transfer process of component M from hot metal to slag, the molar flow in hot metal and that in slag should be equal, i.e. $J_M = J_{\text{MO}_x}$. Specifically, their relationship can be expressed by

$$J_M = F_M \left\{ [\% \text{M}]^b - [\% \text{M}]^* \right\} = F_{\text{MO}_x} \left\{ (\% \text{MO}_x)^* - (\% \text{MO}_x)^b \right\} \quad (15)$$

$$F_M = \frac{k_{im} \rho_m}{100 M_i} \quad (16)$$

$$F_{MO_x} = \frac{k_s \rho_s}{100M_i} \quad (17)$$

Similarly as above, the molar flow of carbon and sulfur should be expressed separately. Namely,

$$J_C = F_C \{ [\%C]^b - [\%C]^* \} = G_{CO} \{ P_{CO}^* / P^\ominus - 1 \} \quad (18)$$

$$J_S = F_S \{ [\%S]^b - [\%S]^* \} = F_{CaS} \{ (\%CaS)^* - (\%CaS)^b \} + F_{Na_2S} \{ (\%Na_2S)^* - (\%Na_2S)^b \} \quad (19)$$

Based on the above equations, the interfacial concentrations of species of both hot metal and slag can be deduced as follows.

$$(\%MO_x)^* = E_M [\%M]^* a_O^{*x} \quad (20)$$

$$(\%MS)^* = E_S [\%S]^* (\%MO)^b a_O^* \quad (21)$$

$$[\%M]^* = \frac{\frac{F_M}{F_{MO_x}} [\%M]^b + (\%MO_x)^b}{\frac{F_M}{F_{MO_x}} + E_M a_O^{*x}} \quad (22)$$

$$[\%C]^* = \frac{\frac{F_C}{G_{CO}} [\%C]^b + 1}{\frac{F_C}{G_{CO}} + \frac{E_C a_O^*}{P^\ominus}} \quad (23)$$

$$[\%S]^* = \frac{F_S [\%S]^b + F_{CaS} [\%CaS]^b + F_{Na_2S} [\%Na_2S]^b}{F_{CaS} E_{CaS} (\%CaO)^b / a_O^* + F_{Na_2S} E_{Na_2S} (\%Na_2O)^b / a_O^* + F_S} \quad (24)$$

The previous equations indicate that the interfacial concentration of all elements dissolved in hot metal can be expressed as a function of bulk concentrations and the interfacial oxygen activity. Then it is possible to define one algebraic equation in terms of only one unknown, the interfacial oxygen a_O^* by performing a mass balance for oxygen.

$$2J_{Si} + 2.5J_P + J_{Fe} + J_{Mn} + J_C - J_S - J_O = 0 \quad (25)$$

This equation can be solved numerically using the initial conditions of hot metal and slag chemical compositions. With this value, the interfacial concentrations of other elements are then computed. It is then possible to compute the new element compositions of hot metal components and of slag species after a time increment (Δt), according to the following equations (26) and (27).

$$\frac{V_m \Delta [\%M]}{\Delta t} = Ak_m \{ [\%M]^* - [\%M]^b \} \quad (26)$$

$$\frac{100 \Delta W_x}{\Delta t} = Ak_s \rho_s \{ (\%M)^* - (\%M)^b \} \quad (27)$$

A computational flow sheet is given in Fig.3 to make the model framework clearer.

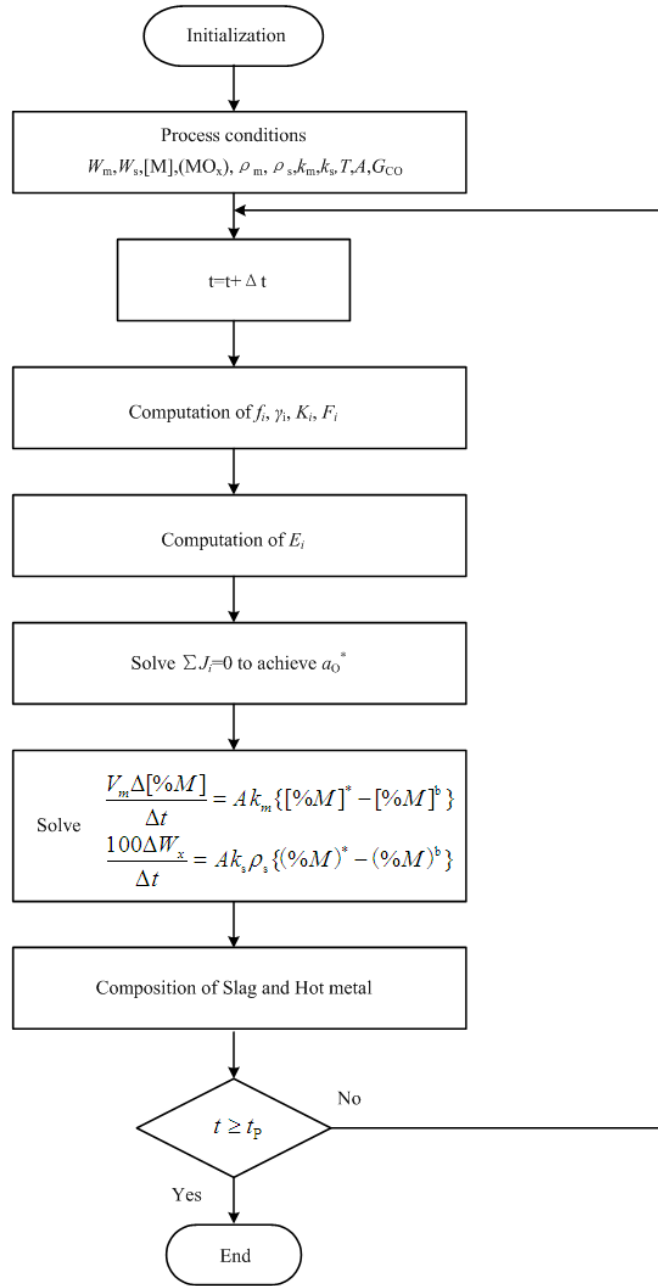


Fig.3 A computational flow sheet of the coupled reaction kinetic model

2.2 Determination of parameters

(1) Equilibrium Constant

The equilibrium constants of reactions considered in the preceding model are as follows [8, 9].

$$\lg K_{Si} = \frac{32000}{T} - 12.29 \quad (28)$$

$$\lg K_{Mn} = \frac{12760}{T} - 5.58 \quad (29)$$

$$\lg K_p = \frac{18425}{T} - 14.53 \quad (30)$$

$$\lg K_{\text{Fe}} = \frac{6340}{T} - 2.745 \quad (31)$$

$$\lg K_{\text{C}} = \frac{1168}{T} + 2.07 \quad (32)$$

$$\lg K_{\text{Si}} = -\frac{5696.06}{T} + 1.532 \quad (33)$$

$$\lg K_{\text{S}_2} = \frac{442.587}{T} - 2.022 \quad (34)$$

(2) Activities of hot metal components

Activities of hot metal components were computed on the basis of the interaction parameter's model proposed by Wagner [10]. Specifically, the activity coefficient of hot metal component i can be expressed by [11]

$$\lg f_i = \frac{1873}{T} \sum_j e_i^j [j] \quad (35)$$

$$\lg f_{\text{C}} = \frac{1873}{T} (0.14[\% \text{C}] + 0.08[\% \text{Si}] - 0.012[\% \text{Mn}] + 0.051[\% \text{P}] + 0.046[\% \text{S}] - 0.34[\% \text{O}]) \quad (36)$$

$$\lg f_{\text{Si}} = \frac{1873}{T} (0.18[\% \text{C}] + 0.11[\% \text{Si}] + 0.002[\% \text{Mn}] + 0.11[\% \text{P}] + 0.056[\% \text{S}] - 0.23[\% \text{O}]) \quad (37)$$

$$\lg f_{\text{Mn}} = \frac{1873}{T} (-0.07[\% \text{C}] - 0.0035[\% \text{P}] - 0.048[\% \text{S}] - 0.083[\% \text{O}]) \quad (38)$$

$$\lg f_{\text{P}} = \frac{1873}{T} (0.13[\% \text{C}] + 0.12[\% \text{Si}] + 0.062[\% \text{P}] + 0.028[\% \text{S}] + 0.13[\% \text{O}]) \quad (39)$$

$$\lg f_{\text{S}} = \frac{1873}{T} (0.11[\% \text{C}] + 0.063[\% \text{Si}] - 0.026[\% \text{Mn}] + 0.029[\% \text{P}] - 0.028[\% \text{S}] - 0.27[\% \text{O}]) \quad (40)$$

(3) Activities of slag species

The regular solution model, first proposed by Lumsden [12], assumes all oxides are present as cations and only one anion, the oxygen ion, distributed randomly. The compounds formed are of the form CaO , FeO , $\text{FeO}_{1.5}$, SiO_2 , $\text{PO}_{2.5}$, $\text{AlO}_{1.5}$, etc.

The molar Gibbs free energy for a regular solution model, incorporating the Darken quadratic formalism, is expressed as follows [13]. The interaction energy between cations of major components in the slag, α_{ij} is given in Table 1.

$$\overline{G}_i^E = \Delta \overline{H}_i = RT \ln \gamma_i \quad (41)$$

$$RT \ln \gamma_i = \sum_j \alpha_{ij} Z_j^2 + \sum_j \sum_k (\alpha_{ij} + \alpha_{ik} - \alpha_{jk}) Z_j Z_k \quad (42)$$

$$Z_i = \frac{n_{i^+}}{\sum n} \quad (43)$$

Table 1 Interaction energy between cations of major components in the slag, α_{ij} (kJ)

$i \quad j$	Fe^{2+}	Fe^{3+}	Mn^{2+}	Ca^{2+}	Mg^{2+}	Si^{4+}	P^{5+}	Al^{3+}
Fe^{2+}	—	-18.66	7.11	-31.38	33.47	-41.84	-31.38	-41
Fe^{3+}	-18.66	—	-56.48	-95.81	-2.93	32.64	14.64	-161.08

Mn ²⁺	7.11	-56.48	—	-92.05	61.92	-75.31	-84.94	-83.68
Ca ²⁺	-31.38	-95.81	-92.05	—	-100.42	-133.89	-251.04	-154.81
Mg ²⁺	33.47	-2.93	61.92	-100.42	—	-66.94	-37.66	-71.13
Si ⁴⁺	-41.84	32.64	-75.31	-133.89	-66.94	—	83.68	-127.61
P ⁵⁺	-31.38	14.64	-84.94	-251.04	-37.66	83.68	—	-261.5
Al ³⁺	-41	-161.08	-83.68	-154.81	-71.13	-127.61	-261.5	—
Na ⁺	19.25	-74.89	80.43	—	—	-111.29	-50.21	—

For the silicate melts which do not completely follow the regular solution model, a conversion factor can be introduced to achieve this correction, i.e. [14]

$$RT \ln \gamma_i = \sum_j \alpha_{ij} Z_j^2 + \sum_j \sum_k (\alpha_{ij} + \alpha_{ik} - \alpha_{jk}) Z_j Z_k + I' \quad (44)$$

The conversion factors of activities employed in present study are given in Table 2 [14].

Table 2 Conversion factors of activities

Reaction	Free energy change (J)
$\text{Fe}_l \text{O}_{(l)} + (1-t)\text{Fe}_{(s \text{ or } l)} = \text{FeO}_{(R.S.)}$	$\Delta G^0 = -8540 + 7.142T$
$\text{SiO}_{2(\beta\text{-tr})} = \text{SiO}_{2(R.S.)}$	$\Delta G^0 = 27150 - 2.054T$
$\text{SiO}_{2(\beta\text{-cr})} = \text{SiO}_{2(R.S.)}$	$\Delta G^0 = 27030 - 1.983T$
$\text{SiO}_{2(l)} = \text{SiO}_{2(R.S.)}$	$\Delta G^0 = 17450 + 2.82T$
$\text{MnO}_{(s)} = \text{MnO}_{(R.S.)}$	$\Delta G^0 = -32470 + 26.143T$
$\text{MnO}_{(l)} = \text{MnO}_{(R.S.)}$	$\Delta G^0 = -86860 + 51.465T$
$\text{Na}_2\text{O}_{(l)} = 2\text{NaO}_{0.5(R.S.)}$	$\Delta G^0 = -185060 + 22.866T$
$\text{CaO}_{(s)} = \text{CaO}_{(R.S.)}$	$\Delta G^0 = 18160 - 23.309T$
$\text{CaO}_{(l)} = \text{CaO}_{(R.S.)}$	$\Delta G^0 = -40880 - 4.703T$
$\text{MgO}_{(s)} = \text{MgO}_{(R.S.)}$	$\Delta G^0 = 34350 - 16.736T$
$\text{MgO}_{(l)} = \text{MgO}_{(R.S.)}$	$\Delta G^0 = -23300 + 1.833T$
$\text{P}_2\text{O}_5(l) = 2\text{PO}_{2.5(R.S.)}$	$\Delta G^0 = 52720 - 230.706T$

Moreover, the activities of CaS and Na₂S which cannot be deduced from the above model, are referenced from literatures [4]. In specific, both γ_{CaS} and $\gamma_{\text{Na}_2\text{S}}$ are set as 5.

(4) Other parameters

Other parameters are set according to the experimental conditions and literatures [1, 2], and listed in Table 3.

Table 3 Data for model calculations

Parameter	Value
ρ_m (kg.m ⁻³)	7000
ρ_s (kg.m ⁻³)	3000
k_m (m.s ⁻¹)	0.0004
k_s (m.s ⁻¹)	0.0002
A (m ²)	0.00159
G_{CO} (mol.mm ⁻² .s ⁻¹)	8×10^{-9}

3. Experimental verification

Industrial purified iron, ferrosilicon, ferrophosphorus, electrolytic manganese and graphite were adopted to prepare the hot metal for dephosphorization experiment by melting in a 10kg medium frequency induction furnace, and the chemical composition of obtained hot metal is given in Table 4. In present work, No.M hot metal was always employed except for the study on effect of Si content on dephosphorization. High oxidation slag samples were used in consideration of the deficiency of oxygen supply during the dephosphorization experiments and their chemical compositions are shown in Table 5. It is notable that No.9 dephosphorization reagent was adopted during the research on effect of Si content on dephosphorization.

Table 4 Chemical composition of hot metal (mass%)

No.	C	Si	Mn	P	S
L	3.78	0.04	0.07	0.42	0.013
M	3.90	0.10	0.30	0.36	0.015
H	4.40	0.48	0.30	0.35	0.03

Table 5 Chemical compositions of initial slags (mass%)

No.	CaO	SiO ₂	Fe ₂ O ₃	Al ₂ O ₃	Na ₂ O	Note
1	24.00	6.00	70.00			
2	31.00	9.00	60.00			
3	30.00		70.00			
4	23.53	5.88	68.63	1.96		No.1+2% Al ₂ O ₃
5	23.08	5.77	67.31	3.85		No.1+4% Al ₂ O ₃
6	22.64	5.66	66.04	5.66		No.1+6% Al ₂ O ₃
7	23.53	5.88	68.63		1.96	No.1+2% Na ₂ O
8	23.08	5.77	67.31		3.85	No.1+4% Na ₂ O
9	22.64	5.66	66.04		5.66	No.1+6% Na ₂ O

The dephosphorization experiments were performed in a 10kg medium frequency induction furnace. The relationships among temperature of the inside of furnace, heating power and heating time were figured out by performing a series of temperature measurement experiments with a rapid response thermocouple of KB type. The temperature of dephosphorization experiment can thus be accurately controlled. In this work, the experimental temperature was set at 1350 °C after the sample was totally melted. 20g slag was then charged into the crucible and a clock was used to keep time in the meantime. The total experimental time was 12 min, and the hot metal was sampled and analyzed in a predetermined time interval.

4. Results and discussion

Both the calculated and experimental results of No.6 and No. 8 were given in Fig.4. It can be seen that the

dephosphorization process has started since the experiment began. The concentration variations of hot metal components such as C, Mn and P were accurately predicted to a large extent. It is worth noting that Si concentration was not analyzed because the desilication reaction was really fast and it was hard to be sampled.

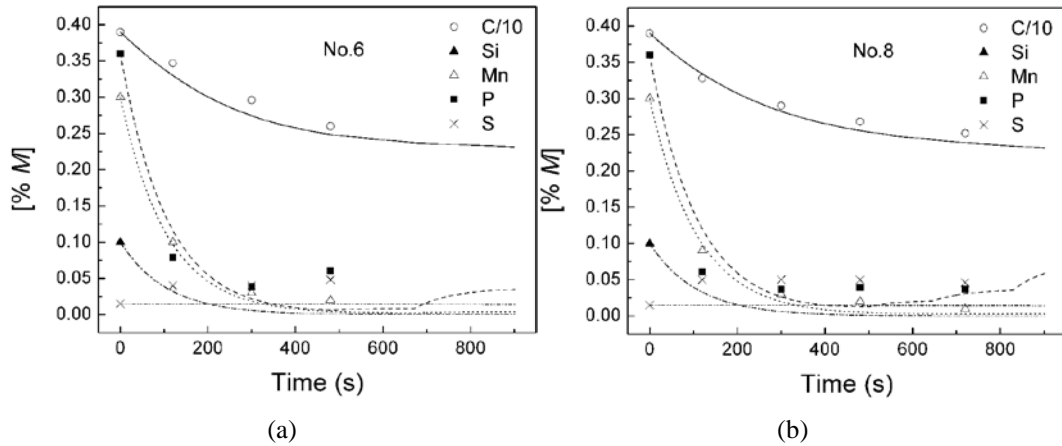


Fig.4 Variation of metal composition with time in run No.6 and No.8

The phosphorus concentration in hot metal during the later stage of experiment is slightly larger than model calculated result. This is probably because some slag adhered to the inwall of small experimental crucible in the later stage and the dephosphorization rate was thus reduced. Also, this might result in the calculated rephosphorization time is later than the experimental one.

Figure 5 shows the relationship between the oxygen activity a_O calculated from the equilibrium of $Fe+O=FeO$ and the model calculated slag-metal interfacial oxygen activity a_O^* . It has been clearly shown that the value of a_O and that of a_O^* are nearly the same when the reaction reaches equilibrium state in the later experimental stage. In the initial stage, the value of a_O^* is much larger than that of a_O and the reaction is thus proved to be proceeded in non-equilibrium state. The whole process is controlled by the mass transfer in slag. Moreover, the difference is getting smaller and smaller with experimental time and the reaction tends to be in equilibrium.

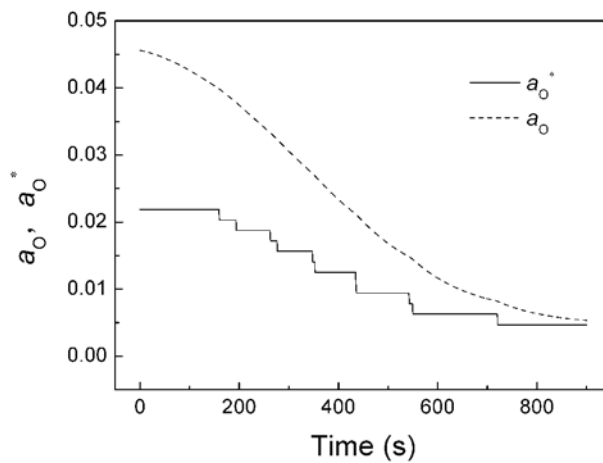


Fig.5 Relationship between a_O and a_O^*

The slag-metal interfacial oxygen activity a_O^* is a decisive factor of coupled reactions and it is related to the slag and

hot metal compositions. Figure 6 illustrates the effects of hot metal and slag compositions on the interfacial oxygen activity a_{O^*} from model calculation. Specifically, the effect of Si concentration in hot metal on the interfacial oxygen activity a_{O^*} can be deduced from Fig.6 (a). It is obvious that a_{O^*} shows a trend of decline as increasing the Si concentration in hot metal. This is reasonable because the interfacial oxygen would be consumed to oxidize the elements such as C, Si and Mn, and which would result in the decrease of interfacial oxygen activity a_{O^*} . It can be observed from Fig.6 (b) that a_{O^*} in both No.2 heat (low FeO) and No.3 heat (low SiO_2) is lower than that in No.1 heat. Besides, the effects of Al_2O_3 and Na_2O on interfacial oxygen activity a_{O^*} can be inferred from Fig.6 (c) and (d). Obviously, the interfacial oxygen activity is barely influenced by the addition of Al_2O_3 and Na_2O . This demonstrates that the key influential factors on interfacial oxygen activity are FeO content in slag and composition of hot metal. It thus can be concluded that a higher content of FeO in slag and lower concentration of C, Si and Mn in hot metal would contribute to a larger value of interfacial oxygen activity. Furthermore, the results indicate that the concentration of Si in the high phosphorus hot metal should be limited at an appropriate value due to the period of dephosphorization is relatively long and the oxidation of silicon is prior to that of phosphorus.

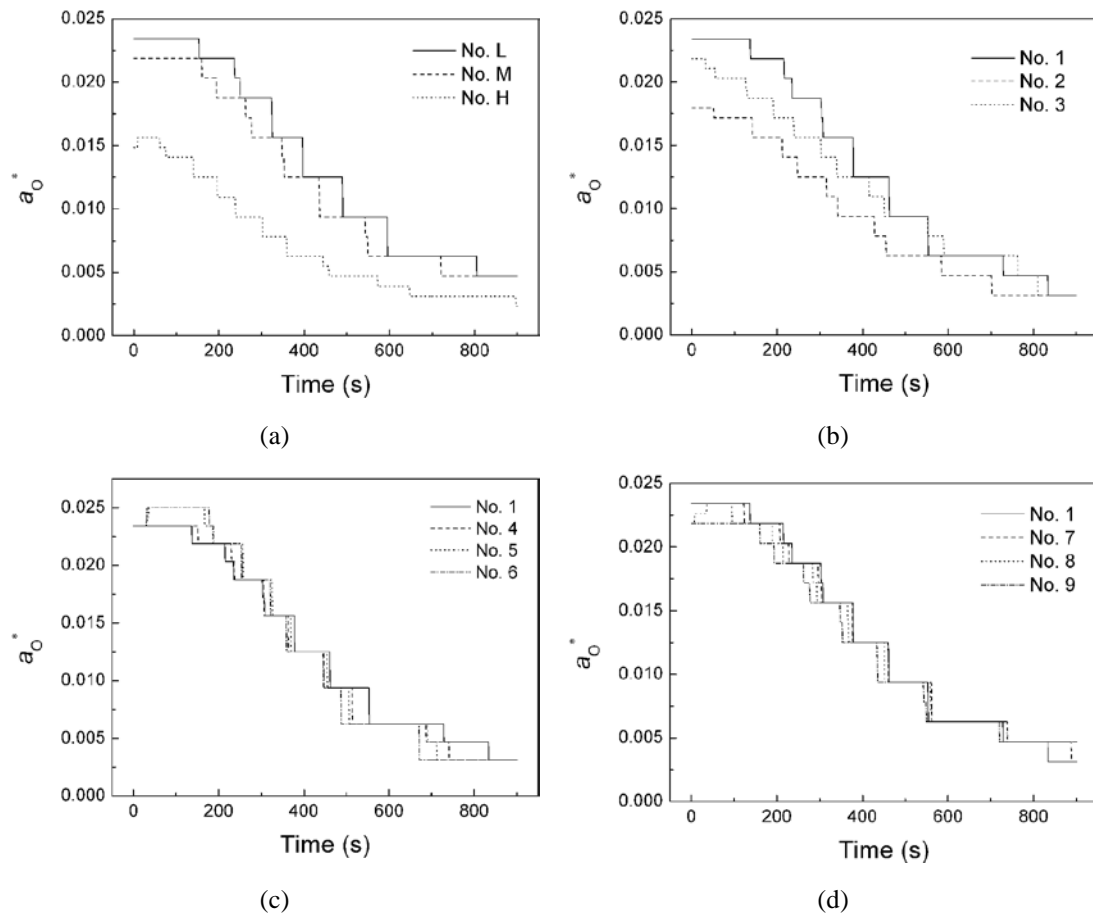


Fig.6 Effects of hot metal and slag compositions on a_{O^*}

In addition, the content variations of slag components can be predicted by the established model and Fig.7 gives the time-dependent slag compositions in No.8 heat. Apparently, the content of FeO remarkably decreases while a gradual rise in content of SiO_2 , P_2O_5 and MnO can be seen. It is notable that the final content of P_2O_5 achieves 9.1% and this

inspires us that the dephosphorization slag produced from duplex steelmaking process is possible to be utilized for the production of phosphate fertilizer.

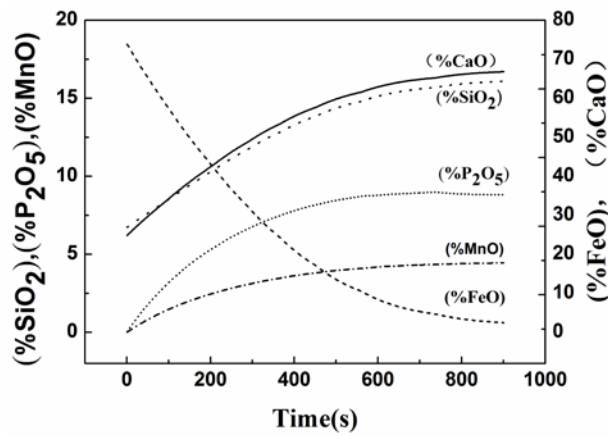


Fig.7 Variations of slag compositions with time

Figure 8 shows the variation of phosphorus concentration and interfacial oxygen activity with time under different slag amounts. As indicated in Fig.8 (a), the dephosphorization rate increases with the rise in slag amount. The minimum phosphorus concentration during dephosphorization is about 0.15% under the slag amount of 8%. But the minimum phosphorus concentration reaches 0.04% and 0.012% respectively when the slag amount is increased to 15% and 21.1%. Also, the tendency of rephosphorization can be reduced when increasing the slag amount.

Additionally, the interfacial oxygen activity decreases with a lower rate if a larger slag amount is employed. This means a larger amount of slag would be beneficial for dephosphorization. However, the amount of slag should be set at a relatively appropriate value due to some economic reasons.

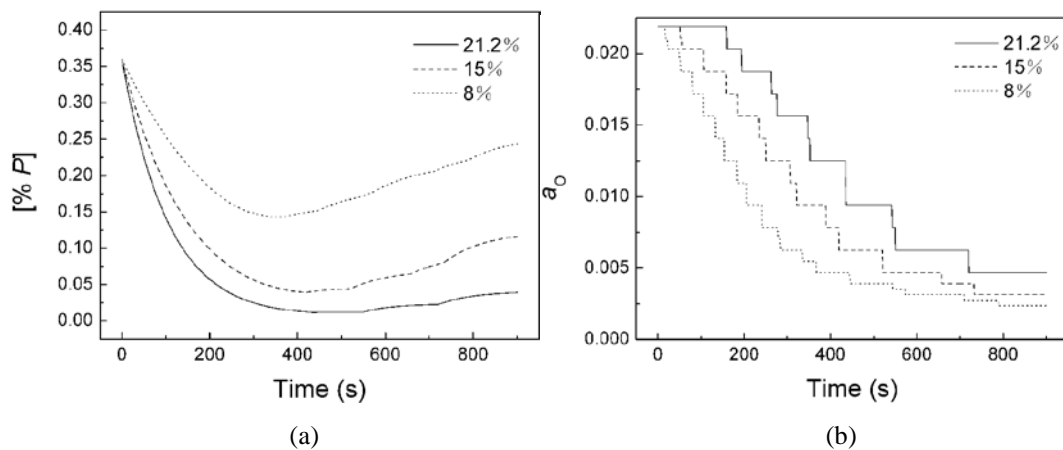


Fig.8 Effect of slag amount on [%P] and a_{O^*}

5. Conclusions

A modified coupled reaction kinetic model is established and validated by the experiments. Furthermore, based on both the calculated and experimental results, the following conclusions can be drawn from present study.

- (1) The coupled reaction kinetics model has been proven to be suitable for the analysis of dephosphorization in

duplex steelmaking process.

(2) The Fe+O=FeO reaction has been turned out to be in non-equilibrium state during the dephosphorization process and tend to reach equilibrium state in the final stage.

(3) A higher content of FeO in dephosphorization slag and lower concentration of C, Si and Mn in hot metal would contribute to a larger value of oxygen activity at the slag-metal interface.

(4) From model calculation, the final content of P₂O₅ in dephosphorization slag achieves 9.1% and this demonstrate the possibility that the dephosphorization slag produced from duplex steelmaking process for high phosphorus hot metal can be utilized for the production of phosphate fertilizer.

(5) A larger amount of slag would be beneficial for dephosphorization. However, the amount of slag should be set at a relatively appropriate value due to some economic reasons.

Nomenclature

Symbols:

K	Equilibrium constant	()	Component in slag	t_p	Total experiment time
a	Activity	p	Pressure	T	Temperature
γ	Activity coefficient of slag component	J	Molar flow	e	Interaction coefficient
X	Molar fraction of slag component	F	Modified mass transfer coefficient	\bar{G}	Molar Gibbs free energy
ρ	Density	k	Mass transfer coefficient	$\Delta\bar{H}$	Molar enthalpy change
M	Molar mass	G_{co}	Rate constant for CO evolution	R	Gas constant
C	Total molar concentration in slag	V_m	Volume of steel	α	Interaction energy
f	Activity coefficient of hot metal component	A	Interfacial area	l'	Conversion factor of activity
E	Modified equilibrium constant	Δt	Time interval	Z	Cationic fraction
[]	Component in hot metal	W	Mass of slag component	n	Moles of cation

Subscript:

m: metal; s: slag; M: component M in hot metal; MO_x: oxide component MO_x in slag; MS: sulphide component in slag.

Superscript:

*: interface; b: bulk.

Acknowledgement

Financial supports from Chongqing Science and Technology Commission (CSTC, 2011BA4018) is greatly appreciated.

References

- [1] D. G. C. Robertson, B. Deo and S. Ohguchi. Multicomponent mixed-transport-control theory for kinetics of coupled slag/metal and slag/metal/gas reactions: application to desulphurization of molten iron. *Ironmaking Steelmaking*, 1984, 11(1), p 41-55.
- [2] S. Ohguchi, D. G. C. Robertson and B. Deo. Simultaneous dephosphorization and desulphurization of molten pig iron. *Ironmaking Steelmaking*, 1984, 11(4), p 202-213.
- [3] Y. Y. Xu, L. C. Zhong. Coupled reaction kinetics of hot metal pretreatment process. *Steelmaking*, 1987, (4), p

63-68.

- [4] Y. C. Dong, H. T. Jiang, Y. Z. Cai. Kinetics on simultaneous dephosphorization and desulphurization from hot metal. *J. N. China Metall. Coll.*, 1993, 10(2), p 7-12, in Chinese.
- [5] J. Fu. Kinetics of steelmaking. Metallurgical Industry Press, Beijing, 2001, in Chinese.
- [6] J. X. Zhao, J. Fu. A coupling dynamic model for oxidizing dephosphorization of stainless steel. *Res. Iron Steel*, 2002, (5), p 13-15, 62, in Chinese.
- [7] Z. H. Tian. Technology and theory of molten steel deep dephosphorization out of converter for production of ultra-low phosphorus steel. PhD thesis, University of Science and Technology Beijing, 2005, in Chinese.
- [8] E. T. Turkdogan. Physical chemistry of high temperature technology. Academic Press, New York, 1980.
- [9] J. X. Chen. Handbook of commonly used diagrams and data in steelmaking process. Metallurgical Industry Press, Beijing, 1984, in Chinese.
- [10] C. Wagner. Thermodynamics of alloys. Adison-Wesley, 1962.
- [11] X. H. Huang. Principles of iron and steel metallurgy. Metallurgical Industry Press, Beijing, 2002, in Chinese.
- [12] J. Lumsden. Physical chemistry of process metallurgy, Part I. Interscience, New York, 1961.
- [13] R. Nagabayashi, M. Hino and S. Ban-ya. Mathematical expression of phosphorus distribution in steelmaking process by quadratic formalism. *ISIJ Int.*, 1989, 29(2), p 140-147.
- [14] S. Ban-ya. Mathematical expression of slag-metal reactions in steelmaking process by quadratic formalism based on the regular solution model. *ISIJ Int.*, 1993, 33(1), p 2-11.